



## Longitudinal dynamic hysteresis in single-domain particles

G. T. Landi and A. D. Santos

Citation: *J. Appl. Phys.* **111**, 07D121 (2012); doi: 10.1063/1.3676416

View online: <http://dx.doi.org/10.1063/1.3676416>

View Table of Contents: <http://jap.aip.org/resource/1/JAPIAU/v111/i7>

Published by the [American Institute of Physics](#).

---

### Related Articles

The role of dipole–dipole interaction in modulating the step-like magnetization of  $\text{Ca}_3\text{Co}_2\text{O}_6$

*J. Appl. Phys.* **111**, 07E133 (2012)

Transmission electron microscopy studies of sintered Nd-Fe-B magnets prepared by cyclic sintering

*J. Appl. Phys.* **111**, 07A720 (2012)

Fully coupled discrete energy-averaged model for Terfenol-D

*J. Appl. Phys.* **111**, 054505 (2012)

Switching behavior of lithographically fabricated nanomagnets for logic applications

*J. Appl. Phys.* **111**, 07B911 (2012)

Structure and magnetic properties of  $\text{Y}_{1-x}\text{Lu}_x\text{FeO}_3$  ( $0 \leq x \leq 1$ ) ceramics

*J. Appl. Phys.* **111**, 053911 (2012)

---

### Additional information on *J. Appl. Phys.*

Journal Homepage: <http://jap.aip.org/>

Journal Information: [http://jap.aip.org/about/about\\_the\\_journal](http://jap.aip.org/about/about_the_journal)

Top downloads: [http://jap.aip.org/features/most\\_downloaded](http://jap.aip.org/features/most_downloaded)

Information for Authors: <http://jap.aip.org/authors>

## ADVERTISEMENT

	<b>Working @ low temperatures?</b> Contact Janis for Cryogenic Research Equipment <a href="http://www.janis.com">Click here</a> to browse our site at <b>www.janis.com</b>	
---	--	---

## Longitudinal dynamic hysteresis in single-domain particles

G. T. Landi<sup>a)</sup> and A. D. Santos

*Instituto de Física da Universidade de São Paulo, 05314-970 São Paulo, Brazil*

(Presented 1 November 2011; received 23 September 2011; accepted 10 November 2011; published online 6 March 2012)

We present results for longitudinal dynamic hysteresis in single domain particles with uniaxial anisotropy. The combined influence of temperature, field-sweeping frequency, and field amplitude is discussed in detail. A novel and efficient numerical method is proposed, based on the direct solution of the infinite hierarchy of differential recurrence relations obtained from averaging over the stochastic realizations of the magnetic Langevin equation. © 2012 American Institute of Physics. [doi:10.1063/1.3676416]

### I. INTRODUCTION

In magnetic nanoparticles the exchange interaction is usually the dominant energy contribution, inhibiting the formation of magnetic domains and forcing all spins to behave in unison,<sup>1</sup> with a single magnetization vector  $\mathbf{M}(t)$ . These materials have been the subject of intensive research for several decades motivated, in parts, by their potential use in applications such as magnetic data storage and magneto-hyperthermia. For systems with uniaxial anisotropy, such as Co or  $\gamma$ -Fe<sub>2</sub>O<sub>3</sub>, the free energy density of the particle may be written as

$$E = -\mathbf{M} \cdot \mathbf{H} - K/M_s^2 (\mathbf{M} \cdot \mathbf{u})^2, \quad (1)$$

where  $\mathbf{H}$  is the externally applied field,  $K$  is the anisotropy constant,  $M_s$  is the saturation magnetization and  $\mathbf{u}$  is the unit vector in the direction of the anisotropy axis, here taken to be parallel to the  $z$ -axis. At zero field, the energyscape Eq. (1) is bistable with two minima separated by a barrier of height  $Kv$ , where  $v$  is the volume of the particle. Due to the small value of  $v$ , this barrier may be of the same order of magnitude as the thermal fluctuations, thus rendering the system as thermally unstable (superparamagnetism).

A robust model to describe the dynamics of single-domain nanoparticles is the Néel-Brown theory<sup>2,3</sup> where Gilbert's equation is augmented with a random field ( $\mathbf{H}_{\text{th}}$ ) to account for the temperature dependence:

$$\dot{\mathbf{M}} = -\gamma_0 \mathbf{M} \times (\mathbf{H}_{\text{ef}} - \eta \dot{\mathbf{M}} + \mathbf{H}_{\text{th}}); \quad (2)$$

here  $\gamma_0$  is the electron's gyromagnetic ratio and  $\eta$  is the dimensionless damping parameter. The first term on the right-hand side corresponds to the effective magnetic field, obtained from the gradient of the free energy (1):  $\mathbf{H}_{\text{ef}} = -\partial E / \partial \mathbf{M}$ . The thermal field is assumed to be a Gaussian white noise, whose Cartesian components ( $i, j = 1, 2, 3$ ) satisfy  $\langle H_{\text{th}_i}(t) H_{\text{th}_j}(t') \rangle = (2k_B T \eta / v) \delta_{ij} \delta(t - t')$ . Here  $k_B$  is Boltzmann's constant and  $T$  is the temperature.

Among the several experiments that are performed in magnetic nanoparticles, one which is of considerable interest

is that of dynamic hysteresis,<sup>4</sup> whose starting point is the application of a harmonic field  $H = H_0 \cos \omega t$ . From the academic standpoint, this problem is important because it allows several conditions to be studied within the same framework by simply modulating  $\omega$  and  $H_0$ . Moreover, from the perspective of applications, this experiment is quite similar to what is done in magneto-hyperthermia cancer treatments,<sup>5</sup> a rapidly progressing field of medical research.

In this paper we study dynamic hysteresis loops in uniaxial single-domain particles. For conciseness, we fix the direction of the applied field to be longitudinal to the anisotropy axis. This preserves the axial symmetry, making it impossible to excite precessional modes of the magnetization. Therefore, the damping enters merely as a multiplicative constant, simplifying the equations involved and reducing the number of parameters necessary to fully describe the system. In Ref. 6 we began this investigation, focusing on the temperature dependence. Here we study the combined influence of temperature, field amplitude and frequency, with particular emphasis on the latter. It is also important to note that albeit being seldom the case in real samples, longitudinal loops are known<sup>4</sup> to encompass several essential features of the problem.

### II. METHODS OF SOLUTION

We work solely with reduced coordinates. Since  $|\mathbf{M}| = M_s$ , we use the unit vector  $\mathbf{m} = \mathbf{M}/M_s$  to describe the magnetization. All magnetic fields are normalized by  $H_A = 2K/M_s$ , which is the maximum coercive force available in the context of the Stoner and Wolfarth model.<sup>1</sup> The effective field becomes  $h_{\text{ef}} = h_0 \cos \omega t + m_z$  and the thermal field now obeys  $\langle h_{\text{th}_i}(t) h_{\text{th}_j}(t') \rangle = \alpha / \sigma \delta_{ij} \delta(t - t')$ . Here  $\alpha = \gamma_0 \eta M_s$  and  $\sigma = Kv/k_B T$ .

Our quantity of interest is the ensemble average of the projection of the magnetization onto the field direction,  $\langle m_z \rangle(t)$ . In spherical coordinates we may write  $m_z = \cos \theta = P_1(\cos \theta)$ , where  $P_n(x)$  are the Legendre polynomials. The noise term in Eq. (2) is multiplicative causing the statistical moments of  $m_z$  to be entangled. On averaging over the stochastic realizations it is possible to show<sup>3</sup> that, in terms of  $p_n(t) = \langle P_n(\cos \theta) \rangle(t)$ , these moments obey the following infinite hierarchy of differential recurrence relations:

<sup>a)</sup>Electronic mail: gtlandi@if.usp.br.

$$\tilde{\tau}_0 \dot{p}_n = \left[ \frac{n(n+1)}{(2n-1)(2n+3)} - \frac{n(n+1)}{2\sigma} \right] p_n + \frac{n(n^2-1)}{4n^2-1} p_{n-2} - \frac{n(n+1)(n+2)}{(2n+1)(2n+3)} p_{n+2} + h \frac{n(n+1)}{2n+1} (p_{n-1} - p_{n+1}), \quad (3)$$

where  $n = 1, 2, \dots$  and  $\tilde{\tau}_0 = (1 + \alpha^2)/(\alpha\gamma_0 H_A)$ . From this equation we construct a system of  $N$  coupled first-order linear ordinary differential equations (ODEs) for the  $p_n$  by defining the column vector  $\mathbb{P} = (p_1, p_2, \dots, p_N)^T$ . We have found that for the present conditions  $N \sim 100$  sufficed to guarantee convergence but, for safety, fixed  $N = 240$ . We may then write

$$\dot{\mathbb{P}} = \mathcal{F}\mathbb{P} + \mathbb{U}, \quad (4)$$

where  $\mathcal{F}$  is a  $N \times N$  matrix and  $\mathbb{U}$  is a column vector of length  $N$ .

To solve systems such as Eq. (4), where the input is harmonic, it is customary to further expand the  $p_n$  in a Fourier series and then solve the resulting system of algebraic equations for the coefficients.<sup>4</sup> In this paper we opted to use a simpler, yet much more powerful approach, which is to solve Eq. (4) directly. The strength of this method lies in the fact that, since Eq. (3) is only a five-term recurrence relation, the resulting matrix  $\mathcal{F}$  — which is also the Jacobian of the ODE system — is remarkably sparse. Powerful integration schemes have been developed to handle such systems,<sup>7</sup> resulting in considerably inexpensive computation times. We also note in passing that this method may be readily extended to the more general case of arbitrary field orientations, the results of which will be published elsewhere.

In this approach both transient and steady-state solutions coexist. However, even though transients are an intrinsic part of the dynamics, in this paper we opted to focus only on the steady-state solutions. The reason is that, in many experiments, it is necessary to average over several cycles of the external field, thus making the role of the transients not entirely clear. To obtain the steady-state solution we begin the integration assuming that the system is in zero-field thermal equilibrium. Then, after each cycle, we verify to what extent the loops have changed with respect to the preceding one. As one might expect, the number of periods required to obtain the final solution increases with increasing frequency or decreasing temperature. While in most conditions only 2 periods are required, in certain cases this value may well surpass 100 periods. Notwithstanding, even in such situations the total integration time remains considerably small, taking on average  $< 1$  s in a simple desktop computer. We believe that this is noteworthy given that the solutions are numerically exact and involve no approximations whatsoever.

### III. RESULTS AND DISCUSSION

Three parameters suffice for a complete description of the problem:  $\sigma \propto 1/T$ ,  $h_0$ , and  $\omega$ , given in units of  $\tau_0 = \tilde{\tau}_0/2$ . We begin the discussion with fixed  $h_0 = 1$ , which corresponds to  $H = H_A$ . In Fig. 1 we present hysteresis loops for a wide

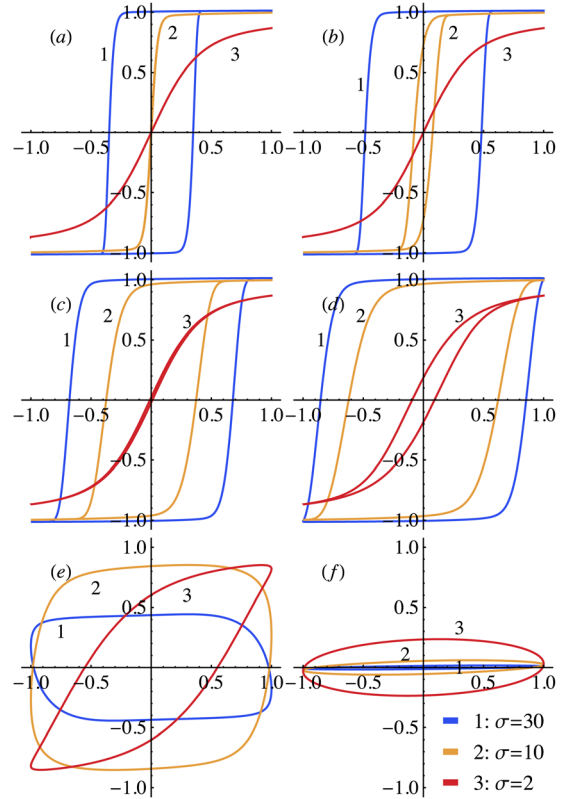


FIG. 1. (Color online) Hysteresis loops with fixed  $h_0 = 1$  and different temperatures: (1)  $\sigma = 30$ , (2)  $\sigma = 10$ , and (3)  $\sigma = 2$ . From (a)–(f):  $\omega\tau_0 = 10^{-7}$ ,  $10^{-5}$ ,  $10^{-3}$ ,  $10^{-2}$ ,  $10^{-1}$ , and 1.

range of frequencies and three different temperatures:  $\sigma = 30$ , 10, and 2, which may be taken as cold, intermediate and hot respectively. Image (a) illustrates quasi-static loops. As it can be seen, only  $\sigma = 30$  is in the ferromagnetic regime with the other two curves showing a superparamagnetic (Langevin-type) behavior. This region is dictated by interwell modes, where the external field promotes the spins with considerable efficiency over the anisotropy barrier ( $m_z = 0$ ). Thence, except for  $\sigma = 2$  where the strong thermal fluctuations inhibit the alignment of the spins with the external field, the loops saturate. Hysteresis is, in parts, related to ferromagnetic order which should occur if the measurement time — viz.,  $2\pi/\omega$  — is smaller than the relaxation time of the particle. An example of such is seen by comparing Figs. 1(a) and 1(b) when  $\sigma = 10$  (orange curve).

In the Stoner and Wolfarth model, where neither the temperature nor the frequency are relevant, the longitudinal loops are perfect squares with coercivity  $h_c = 1$ . In Fig. 1 it can be seen that  $h_c$  remains well below this value for all  $\sigma$  and  $\omega$  (except at high frequencies; see below). This means that even at very low temperatures, the shallower potential minima may be completely depleted well before the bistable character is destroyed (*depletion effect*<sup>3</sup>).

In Fig. 1(d), the curve for  $\sigma = 2$  begins to show a non-zero coercivity, even with the loops still being unable to saturate. This hysteresis is caused by an effect known as *gyromagnetic response*, related to the restriction  $|\mathbf{M}| = M_s$ , which forces the magnetization to precess on a sphere of radius  $M_s$ . Therefore, as the frequency is increased, it becomes

unable to follow the external field. For instance, note that even though the curves for  $\sigma = 10$  and  $30$  are still able to saturate [Fig. 1(d)], they are already remarkably wide. This effect is further enhanced in Figs. 1(e) and 1(f). At this point the external field is no longer capable of efficiently promoting the spins over the equatorial barrier. Therefore, the interwell modes are replaced by a perturbative intrawell motion, near the equilibrium positions  $m_z = \pm 1$ . Note also that, as a consequence, the loops at high temperatures become taller.

An interesting phenomena is observed in Fig. 1(e) for  $\sigma = 30$  (blue curve), where the hysteresis loop is tilted to the left meaning that  $\mathbf{M}(t)$  and  $\mathbf{H}(t)$  are out-of-phase. This is commonly seen in ferromagnetic resonance experiments which, however, cannot be the case in the current problem since the precessional modes of the magnetization vanish from Eq. (2) whenever axial symmetry is preserved. In fact, this is the last step before the intrawell modes become dominant. In order to further understand this effect we introduce a remarkably useful parameter, which we refer to as the “coercive time” ( $t_c$ ). While the coercive field ( $h_c$ ) is defined from the  $m(h)$  plots such that  $m(h_c) = 0$ , the coercive time is computed from the  $m(t)$  curve such that  $m(t_c) = 0$ . Note that, since  $h = h_0 \cos \omega t$ ,  $h_c$  is limited by the value of  $h_0$  and contain no information about the time-dependent dynamics [obviously,  $h_c = h(t_c)$ ]. For instance, the loops for  $\sigma = 30$  in Figs. 1(d) and 1(e) are completely different but, notwithstanding, have similar  $h_c$ . We define  $t_c$  as corresponding to the crossing from the second to third quadrants, where  $h < 0$ ; that is  $\omega\pi/2 \leq t_c \leq \omega 3\pi/2$ . However, for comparative purposes it is convenient to drop the dependence on  $\omega$ , thus taking it as ranging between  $\pi/2 \leq t_c \leq 3\pi/2$ . With this definition we have that if  $t_c = \pi/2$  there is no hysteresis, as in the superparamagnetic case, whereas if  $t_c = \pi$  we have reached the maxima  $h_c = h_0$ .

In the vast majority of cases the reversal occurs at  $\pi/2 \leq t_c \leq \pi$ , since the thermal fluctuations facilitate the promotion. However, there is nothing that restricts it from occurring at the complementary interval and, albeit unlikely, this is precisely what happens in Fig. 1(e). This effect comes from a delicate balance between  $\sigma$  and  $\omega$ , where the thermal fluctuations assist the external field in promoting reversals that it would otherwise be unable to. In Fig. 2(a) we present results for  $t_c \times \omega$  where it can be seen that this effect manifests itself for both  $\sigma = 10$  and  $30$ , remaining only during a short frequency interval of roughly one decade, which is also sensitive to the value of  $\sigma$ . The usefulness of  $t_c$  becomes clear from this image, in the sense that it encompasses all properties of  $h_c$ , plus information related to the relative phase between  $\mathbf{M}(t)$  and  $\mathbf{H}(t)$ .

We now lift the restriction of  $h_0 = 1$ . In Fig. 2(b) we present, for fixed  $\sigma = 10$ , curves of  $t_c \times \omega$  for 19 values of  $h_0$ , ranging from 0.01 to 1.0 in logarithmic steps. The transition from the linear to the nonlinear response regimes is clearly visible, taking place between  $h_0 = 0.1$  and  $0.2$  (this curve is marked with an asterisk). For all conditions,  $t_c$  has a distinct maxima followed by a minima. At very low frequencies, spin reversals occur with relative ease, independent of  $h_0$ . However, as  $\omega$  increases, a stronger field becomes necessary and therefore the reversal tends to take place near

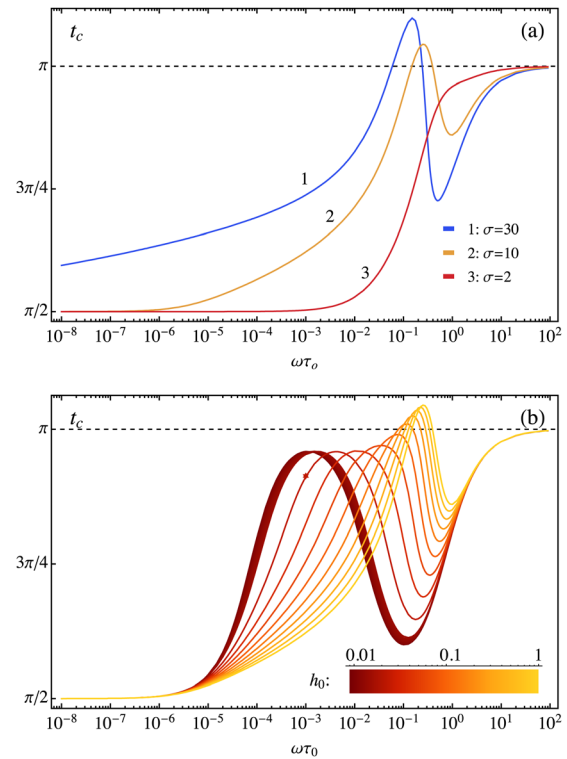


FIG. 2. (Color online) Coercive time as a function of frequency. (a) fixed  $h_0 = 1$  and different values of  $\sigma$ ; (b) fixed  $\sigma = 10$  and different values of  $h_0$ .

$t_c = \pi$  (where  $h$  is a minimum). Afterwards, these modes are eventually replaced by intrawell modes, which causes  $t_c$  to gradually diminish. Notwithstanding, at sufficiently high frequencies the gyromagnetic response becomes important and, therefore,  $t_c$  begins to rise once again, this time indefinitely, toward it is asymptote  $t_c \rightarrow \pi$ . Above  $h_0 = 0.2$ , both extrema get shifted to higher frequencies and, after  $h_0 = 0.7$ , the  $t_c = \pi$  threshold is surpassed. It is quite interesting to note that this effect can now be seen to be nothing but the maxima in  $t_c$ , which is gradually being shifted to higher frequencies as  $h_0$  increases.

In conclusion, we have discussed longitudinal dynamic hysteresis loops in single-domain particles, treating all free parameters of the system. The simulations cover an extensive range of conditions, which was made possible by the remarkable efficiency of the algorithms employed.

This paper was funded by the Brazilian funding agencies FAPESP and CNPq.

<sup>1</sup>E. Stoner and E. Wohlfarth, *Philos. Trans. R. Soc. London, Ser. A* **240**, 599 (1948).

<sup>2</sup>W. Brown, *Phys. Rev.* **130**, 1677 (1963) <http://link.aps.org/doi/10.1103/PhysRev.130.1677>.

<sup>3</sup>W. Coffey, Y. P. Kalmykov, and J. Waldron, *The Langevin Equation. With Applications to Stochastic Problems in Physics, Chemistry and Electrical Engineering*, 2nd ed. (World Scientific, Singapore, 2004), p. 678.

<sup>4</sup>I. Poperechny, Y. Raikher, and V. Stepanov, *Phys. Rev. B* **82**, 174423 (2010).

<sup>5</sup>Q. A. Pankhurst, N. K. T. Thanh, S. K. Jones, and J. Dobson, *J. Phys. D: Appl. Phys.* **42**, 224001 (2009).

<sup>6</sup>G. T. Landi, *J. Magn. Magn. Mater.* **324**, 466–470 (2012).

<sup>7</sup>A. C. Hindmarsh, P. N. Brown, K. E. Grant, S. L. Lee, R. Serban, D. A. N. E. Shumaker, and C. S. Woodward, *ACM Trans. Math. Softw.* **31**, 363 (2005).